

565 **Appendix**

566 Diverse, multi-modal behaviors generated by our models on different environment are best experi-
567 enced and understood in a video. We invite you to visit <https://submission0.github.io> to see
568 BeT models in action.

569 **A Environment and Dataset Details**

570 **Point mass environments:** In the point mass environment, we have a simple point-mass agent
571 with two-dimensional observation and action spaces. The observation of the agent denotes the (x, y)
572 position of the agent, while the action sets the immediate $(\Delta x, \Delta y)$ displacement of the agent in the
573 next timestep.

574 To show the effects of unimodal and multimodal behavioral cloning algorithms more cleanly, we
575 also add a "snapping" effect to the environment which moves the agent close to the nearest integer
576 coordinates after each step.

577 We generate random trajectories for each of our Multipath experiment datasets.

- 578 1. In the first one (Fig. 2), our dataset has two modes, which are colored differently in the
579 figure based on the path taken at the fork.
 - 580 (a) In the first set of demonstrations, the point mass follows the trajectory
581 $(1, 2), (2, 2), (2, 3), (2, 4), (3, 4), (4, 4), (4, 3), (4, 2), (5, 2)$.
 - 582 (b) In the second set of demonstrations, the point mass follows
583 $(1, 2), (2, 2), (2, 1), (2, 0), (3, 0), (4, 0), (4, 1), (4, 2), (5, 2)$.
- 584 2. For the second Multipath environment (Fig. 5), there are three modes of demonstration,
585 which are colored in the figure according to their first step direction.
 - 586 (a) In the first set of demonstration, the point mass follows $x = y$ from $(0, 0)$ to $(8, 8)$ with
587 $\sqrt{2}$ size step increments.
 - 588 (b) In the second set of demonstration, the point mass follows straight lines from $(0, 0) \rightarrow$
589 $(0, 4) \rightarrow (4, 4) \rightarrow (8, 4) \rightarrow (8, 8)$ with step size 1.
 - 590 (c) In the third set of demonstration, the point mass follows straight lines from $(0, 0) \rightarrow$
591 $(4, 0) \rightarrow (4, 4) \rightarrow (4, 8) \rightarrow (8, 8)$ with step size 1.

592 **CARLA environment:** We use the CARLA [19] self-driving environment to examine BeT perfor-
593 mance in environments with high-dimensional observation spaces. CARLA uses the Unreal Engine
594 to provide a photo-realistic driving simulation. We create our environment on the Town04 map in
595 CARLA 0.9.13. The observation space is $224 \times 224 \times 3$ RGB images from the vehicle, which are
596 processed by an ImageNet-pretrained, frozen ResNet-18 to a 512-dimensional real-valued vector.
597 The action space is $[-1, 1]^2$ with an accelerator-brake axis and a steering axis.

598 The dataset on this environment is collected with the built-in PID agent with minor tuning. We fix
599 waypoints in the trajectory that the demonstration agent needs to follow. The waypoints fork around
600 two central blocks: one set of trajectories thus go to the left, while another set of demonstration
601 trajectories go to the right. While collecting the demonstrations, we add some noise in the environment
602 before executing an action so that there is some variation in the set of 100 total demonstrations that
603 we collect in the environment.

604 We do not introduce any traffic participants in this environment intentionally as we intend to show
605 the effects of cleanly bi-modal distributions on the learning algorithms in an environment more
606 complicated than the point-mass environments.

607 **Block-push environment:** We use a simulated environment similar to Multimodal Push environ-
608 ment described in [23]. We take the environment implementation directly from the PyBullet [14] based
609 implementation provided by Florence et al. [23] in [https://github.com/google-research/](https://github.com/google-research/ibc/tree/master/environments)
610 [ibc/tree/master/environments](https://github.com/google-research/ibc/tree/master/environments).

611 In our environment, an XArm robot is situated in front of two blocks in a 0.75×1 plane. On the
612 plane there are also two square targets. The goal of the agent is to push the blocks inside of the

613 squares. However, the exact order of the block being pushed, or the combination of which block is
614 pushed in which square doesn't matter. A block is considered successfully pushed if the center of the
615 block is less than 0.05 away from a square.

616 On initialization, the blocks' positions are randomly shifted within a rectangle of side lengths
617 (0.2, 0.3), while the squares are randomly shifted within a rectangle of size (0.01, 0.015). Addition-
618 ally, the blocks were rotated at an uniformly arbitrary angle, while the target squares were rotated at
619 an angle between $(\frac{\pi}{6}, -\frac{\pi}{6})$.

620 The demonstrations in this environments were collected with a hard-coded controller. There are two
621 modes of multimodality inherent in the controller generated demonstrations. The controller:

- 622 1. Selects a block to start pushing first,
- 623 2. At the same time, independently chooses a target for the block to be pushed into.
- 624 3. Once the first block is pushed to a target, it pushes the second block to the remaining target.

625 Thus combinatorially, the controller is capable of four different modes of behavior. There are
626 additional stochasticity in the controller behavior since there are many ways of pushing the same
627 block into the same target.

628 The controller pushes the blocks to their targets following specific behavior primitives, such as
629 moving to origin position, moving to a place collinear with a block and its target, and making a
630 straight motion from that position towards the target unless the block rotates too much from its
631 starting position.

632 Our models were trained on 1,000 demonstrations, all generated from the controller under the above
633 randomized modes.

634 **Franka kitchen environment:** For the final set of experiments, we use the Franka Kitchen envi-
635 ronment originally introduced in the Relay Policy Learning [30] paper. In that paper, the authors
636 introduce a virtual kitchen environment where human participants in VR manipulated seven different
637 objects in the kitchen: one kettle, one microwave, one sliding door, one hinged door, one light switch,
638 and two burners. In total, we use 566 demonstrations collected by the researchers in that paper, where
639 in each demonstration episode, each participant performed four manipulation task specified by the
640 researchers in advanced.

641 The manipulator agent in simulator is a Franka Emika Panda robot, which is controlled through a 9-
642 dimensional action space controlling the robot's joint and end-effector position. The 60-dimensional
643 observation space is split into two parts, the first 30 dimension contains information about the
644 current position of the interesting factors in the environment, while the last 30 dimensions contain
645 information about the goal of the demonstrator or the agent. Note that in our demonstrations and our
646 environments, we zero out the last 30 dimensions in all cases since we assume goal is not labelled in
647 the demonstrations and is not specified in the unconditioned rollouts of the model.

648 One thing to note that, while the D4RL [24] paper also has three versions of the dataset, we chose
649 to use the original version of the collected data from the Relay Policy Learning [30] paper. That
650 is because the relay policy learning dataset is not labeled with intended tasks of the participants or
651 rewards, while the D4RL dataset is geared towards that.

652 B Implementation Details and Hyperparameters

653 B.1 Baselines

654 **Multi-layer Perceptron with MSE** For our MLP with MSE baselines, we trained fully connected
655 neural networks with optionally BatchNorm layers. In each of our environment, we varied the depth
656 and the width of the MLPs to fit them best according to the bias-variance trade-off, while training
657 them on 95% of the dataset and testing on the remaining 5% on the dataset in terms of MSE loss.

658 **Nearest Neighbor** Nearest Neighbor is conceptually the simplest baseline we show in this paper.
659 During training, our Nearest Neighbor model simply stores all the (o, a) pairs. During test time,

660 given a query observation, o , we find the observation o' with the minimum Euclidean distance to that
661 in the representation space, and execute the associated action a' in the environment.

662 While it is a simple baseline, we show that it has a surprisingly high effectiveness in simple envi-
663 ronments like CARLA, or dense environments like Kitchen where there is less of a chance in going
664 OOD simply by executing seen actions. On the other hand, in environments like Block-push where
665 the model needs to interpolate or extrapolate more, the NN model fails more.

666 **k-Nearest Neighbor with Locally Weighted Regression** A slightly more robust version of NN for
667 regression problems, k-NN with locally weighted regression or LWR, is the next baseline we use. In
668 this baseline, we take the k-nearest neighbors (in all our cases, 5) in the observation representation
669 space, and take a weighted average of their associated actions. The weighting is based on the negative
670 exponent of the distance, or namely, $\exp -||o - o'||$, as seen in [56]. This model is better than simple
671 Nearest Neighbors in interpolations, and thus we see a higher success in the Kitchen environment.

672 **Continuous Generative Model: VAE with Gaussian Prior** Following prior works[60], we use
673 variational auto-encoders (VAE) for encoding and decoding sequences of actions into a smaller latent
674 space. The VAE here learns to compress a sequence of $T = 10$ actions into a single latent variable z
675 of 10 dimensions. The hyperparameters for training the VAE has been taken directly from Pertsch
676 et al. [60].

677 Concurrently with training the VAE, we train a state-conditioned latent prior model that tries to predict
678 $P(z | o)$. This latent generator produces a vector of μ and σ which is sampled to find latent z , and
679 we feed a Gaussian distributed variable z back into the decoder network where the action sequence
680 is reconstructed. For the current observation o_t , sequence of reconstructed actions a_t, \dots, a_{t+9} are
681 performed in a simulated environment.

682 The design choices of this algorithm has been heavily inspired by [60]. Although this model shows
683 promise in theory, we found in practice that unconditional rollout from this model is not very
684 successful. We believe the shortcoming is a result of random sampling from the z space that does not
685 take into account the recently executed actions, and using a single-mode Gaussian as the state prior
686 similar to [60], and thus this baseline is only slightly better than the MLP-MSE model.

687 **Continuous Generative Models: Normalizing Flow with and without Prior** Similar to Singh
688 et al. [70], we use a Normalizing Flow [18] based generative model. We follow the architectural
689 choices and the hyperparameters from [70] in our baseline implementation.

690 Our observation-conditioned Flow model is trained on the distribution $P(a | o)$ to continuously
691 transform it into an identity Gaussian distribution of the same dimensions as a . To find a better prior
692 than simply an identity Gaussian, we also trained a prior model that generates μ, σ of a Gaussian
693 distribution given the observation o . We found that the prior improves the quality of the rollouts,
694 however slightly.

695 We believe the under-performance of these continuous generative approaches were based on two
696 major problems. One is that they fail to take historical context in concern, and by being a continuous
697 distribution, returned less likely actions that led to more rollouts going OOD. Second, they were
698 designed with a focus of making RL approachable by compressing the action space, which requires
699 having a prior that is not so strict. However, most of BeT’s performance comes from having a strong
700 prior over the actions, which is only augmented by the action offset prediction.

701 **Implicit Behavioral Cloning** Implicit Behavioral Cloning (IBC) [23] takes a different approach in
702 behavioral cloning, where instead of learning a model $f(o) := a$, we learn an energy based model
703 $E(o, a)$ where the intended action a at any observation is defined as $\arg \min_a E(o, a)$. While this
704 suffers from all the classic issues of training an EBM, like higher sample complexity and higher
705 complexity in sampling, IBC models have been shown to have higher success in learning multi-modal
706 and discontinuous actions.

707 As a baseline, we use the official implementation provided in [https://github.com/
708 google-research/ibc](https://github.com/google-research/ibc) For the CARLA environment, we use equivalent hyperparameters from the
709 “pushing from pixels” hyperparameters. For the Block-pushing environment, we use the “pushing
710 from states” hyperparameters. Finally, for the Kitchen environment, we use the “D4RL kitchen”
711 hyperparameters.

712 While IBC is our strongest baseline, in our experience it is also one that is quite easy to overfit to
 713 our datasets. As a result, we monitored test performance over the training and had to employ early
 714 stopping for both the CARLA and the Block-pushing tasks.

715 **Trajectory Transformers** Trajectory Transformers [35], especially the variant that is trained
 716 without any rewards only on states and actions from demonstrations, seem similar to our approach,
 717 there are a few crucial differences. While we agree that BeT and Trajectory Transformer based
 718 behavior cloning both use some type of discretization to fit demonstration datasets with a minGPT,
 719 we believe that is where the similarities end. The primary differences between the algorithms is
 720 in our design choices: namely what distributions they model, and consequently how they treat the
 721 observations. The differences are explained more thoroughly below.

- 722 • **Modeled distribution:** From a provided set of demonstrations, trajectory transformers
 723 model the joint distribution $P(\text{action}, \text{observations})$. On the other hand, BeT models the
 724 conditional distribution $P(\text{action} | \text{observations})$. Modeling the joint distribution requires
 725 MinGPT to model the forward dynamics of the environment, which can be arbitrarily
 726 difficult based on the environment.
- 727 • **Observation discretization:** Because trajectory transformers have to model the observations
 728 as well, it needs to discretize the observation space. As a result, TT cannot extend to high
 729 dimensional observational spaces, such as visual observations. This limitation is also
 730 acknowledged by the authors of Trajectory Transformers. BeT, on the other hand, does
 731 not model the observations and thus does not need to discretize them. Thus BeT can
 732 scale to arbitrarily high dimensional observations, as we show in the CARLA environment
 733 experiments, where BeT learns behaviors from high dimensional visual observations.
- 734 • **Efficient historical encoding:** Trajectory transformer encodes each (state, action) pair into
 735 a total of $|S| + |A|$ input/output tokens, while BeT encodes them into one input/output token.
 736 On a base MinGPT implementation that means a $O((|S| + |A|)^2)$ efficiency gain for BeT, or
 737 for example 4761x less compute for the same historic context in the Kitchen environment.

738 As a baseline, we trained and rolled out Trajectory Transformer on the Kitchen environment.
 739 It failed to complete any tasks for unconditioned, greedy, or beam search rollouts. We would
 740 like to note that the Kitchen environment is more complicated than the MuJoCo environments
 741 (HalfCheetah, Hopper, Walker2d, and Ant) that the paper experimented on. At the same time,
 742 this environment has an order of magnitude fewer samples on the training set (10^6 vs. approx-
 743 imately 120k). We tried both our own implementation and the implementation from <https://github.com/Howuhh/faster-trajectory-transformer>
 744 with the recommended parameters for the AntMaze environment, which is the largest environment used by the authors.

746 B.2 Algorithm Details

747 **Loss function details:** In this paper, we use two loss functions that are inspired by practices in
 748 computer vision, in particular object detection. The first of them is the Focal loss [44], and the second
 749 one is the Multi-task loss [26].

750 The Focal loss is a simple modification over the cross entropy loss. While the normal cross entropy
 751 loss for binary classification can be thought of $\mathcal{L}_{ce}(p_t) = -\log(p_t)$, the Focal loss adds a term
 752 $(1 - p_t)^\gamma$ to this, to make the new loss

$$\mathcal{L}_{focal}(p_t) = -(1 - p_t)^\gamma \log(p_t)$$

753 This loss has the interesting property that its gradient is more steep for smaller values of p_t , while
 754 flatter for larger values of p_t . Thus, it penalizes and changes the model more for making errors
 755 in the low-probability classes, while is more lenient about making errors in the high probability
 756 classes. Using this error in the object detection world has helped with class imbalance between
 757 different classes, and here it helps BeT learn to predict different k -means from the dataset even if
 758 their appearance in the dataset is not completely balanced.

759 For the multi-task loss, we use the formulation

$$\text{MT-Loss} \left(\mathbf{a}, \left(\langle \hat{a}_i^{(j)} \rangle \right)_{j=1}^k \right) = \sum_{j=1}^k \mathbb{I}[\mathbf{a}] = j \cdot \|\langle \mathbf{a} \rangle - \langle \hat{a}^{(j)} \rangle\|_2^2$$

760 This helps us penalize only the offset for the ground truth class, thus making sure the MinGPT is not
 761 trying to predict the right action offset through all classes and instead only trying to predict the action
 762 offset through the right class.

763 In practice, we optimize the combined loss, $\mathcal{L}_{focal} + \alpha\mathcal{L}_{mt}$ while α is a hyperparameter that just
 764 makes sure at initialization the two losses are of the same order of magnitude.

765 **Compute details:** All of our code was run in a single NVIDIA RTX 3080 GPU for state-based
 766 environments and RTX 8000 for image-based environments.

767 **Performance measurement details:** We measured the performance reported in the Section 3.5 in
 768 an NVIDIA RTX 3080 machine with AMD Threadripper 5950x CPUs. We took the average over
 769 three runs to minimize inter-run variances, and measured wall-clock time to report in the paper.

770 In terms of raw computation time to determine one action from the observations, in the Kitchen
 771 environment, BeT took 2.8 ms, while IBC took 52 ms and MLP, as the fastest point of comparison,
 772 took 0.5 ms. On the same environment, a single step of Trajectory Transformer took 867.86 ms, on
 773 an implementation that used more advanced tricks such as attention caching.

774 **Hyperparameters list:** We present the BeT hyperparameters in Table 4 below:

Table 4: Environment-dependent hyperparameters in BeT.

Hyperparameter	Point-mass	CARLA	Block-push	Kitchen
Layers	1	3	4	6
Attention heads	2	4	4	6
Embedding width	20	256	72	120
Dropout probability	0.1	0.6	0.1	0.1
Context size	2	10	5	10
Training epochs	10	40	350	50
Batch size	64	128	64	64
Number of bins k	2; 3	32	24	64

775 However, we have found that as long as the model does not overfit, a wide range of parameters all
 776 yield favorable results for BeT; thus, this table should be taken as reference values for reproducing
 777 our results rather than the only parameter sets that work.

778 Apart from that, we have some hyperparameters that are shared across all BeT experiments. They are
 779 reproduced in Table 5.

Table 5: Shared hyperparameters for BeT training

Name	Value
Optimizer	Adam
Learning rate	1e-4
Weight decay	0.1
Betas	(0.9, 0.95)
Gradient clip norm	1.0

780 B.3 Pseudocode

781 See the pseudocode described on Algorithm 1.

782 B.4 Architecture and Implementation

783 For our implementation, we used the MinGPT [36] repository almost as-is. We modified the input
 784 token conversion layer to a linear projection layer to handle our continuous, instead of discrete, inputs.
 785 Apart from that, we followed the MinGPT architecture quite exclusively, with successive attention
 786 layers with a number of attention head and embedding dimensions. Between the layers, we used
 787 dropout regularization same as [36].

Algorithm 1 Learning Behavior Transformer from a dataset of behavior sequences.

Input: Dataset $(o_{t,i}, a_{t,i})_{t,i}$ for $0 \leq i \leq$ number of demonstrations, $0 \leq t \leq$ maximum episode lengths, intended number of clusters k and context history length h .

Initialize: θ_M the parameters for MinGPT, $\{A_i\}_{i=1}^k$ cluster centers randomly in the action space.

Learn k-means encoder/decoder:

Using all possible $a_{t,i}$, learn the k cluster centers using the k means algorithm.

Set $\{A_i\}_{i=1}^k$ as the learned cluster centers.

Define functions:

$$\lfloor a \rfloor := \arg \min_{i=1}^k \|a - A_i\|$$

$$\langle a \rangle = a - \lfloor a \rfloor$$

$$\text{Enc}(a) = (\lfloor a \rfloor, \langle a \rangle)$$

$$\text{Dec}(\lfloor a \rfloor, \langle a \rangle) = A_{\lfloor a \rfloor} + \langle a \rangle$$

Train MinGPT trunk of BeT:

while *Not converged* **do**

 Sample trajectory subsequence $(o_t, a_t), \dots, (o_{t+h-1}, a_{t+h-1})$ from the dataset.

 Feed in the observations $(o_t, o_{t+1}, \dots, o_{t+h-1})$ into the MinGPT.

 Get categorical distribution probabilities $p_{\tau,c}$ for $t \leq \tau \leq t+h-1, 1 \leq c \leq k$.

 Compute focal loss \mathcal{L}_{ce} of $p_{\tau,c}$ against ground truth class $\lfloor a_\tau \rfloor$, for all τ, c .

 Get the residual action offset per class, $\langle a_{\tau,c} \rangle$, for all τ, c from MinGPT.

 Calculate the multi-task loss, \mathcal{L}_{mt} , against true class predicted offset, $\sum_{\tau} \|\langle a_{\tau, \lfloor a_\tau \rfloor} \rangle - \langle a_\tau \rangle\|_2^2$

 Backprop using the normalized loss, $\mathcal{L}_{ce} + \alpha \mathcal{L}_{mt}$ where α makes the losses of equal magnitude.

Running on the environment:

while *Episode not completed* **do**

 Stack the last h observations in the environment, $(o_t, o_{t+1}, \dots, o_{t+h-1})$ and feed into MinGPT.

 Get categorical probabilities $p_{\tau,c}$ for $t \leq \tau \leq t+h-1, 1 \leq c \leq k$ from the MinGPT.

 Sample a class c from $p_{t+h-1,c}$ for $1 \leq c \leq k$.

 Get the associated action offset, $\langle a_{t+h-1,c} \rangle$ from the MinGPT.

 Decode into full continuous action, $\bar{a}_{t+h-1} := \text{Dec}(c, \langle a_{t+h-1,c} \rangle)$

 Execute decoded action \bar{a}_{t+h-1} into environment.

788 For the smallest tasks, like point-mass environments, we used models with approximately 10^4
789 parameters, which went up to around 10^6 for Kitchen environments.

790 C Ablation studies

791 In this section, we provide more details about the ablation studies presented in the main paper, as
792 well as present detailed plots of our ablation studies that compare different versions of the BeT
793 architecture.

794 C.1 Ablating historical context

795 One of the reasons why we used transformer-based generative networks in our work is because of
796 our hypothesis that having historical context helps our model learn better behavioral cloning. Our
797 experiments are performed by using the same model and simply providing sequences of length one
798 on training and test time. As we can see on Sec. 3.5, having some historical context helps our model
799 learn much better.

800 C.2 Ablating the number of discrete bin centers, k

801 Since BeT is trained with a sum of focal loss for the binning head and MSE loss for the offset head,
802 the number of cluster centers present a trade-off in the architecture. Concretely, as the number of bins

803 go up, the log-likelihood loss goes up but the MSE loss goes down. In Sec. 3.5, we showed that using
804 only one bin ($k = 1$) decreases the performance level of BeT.

805 In this section, we present the plot of the variation in performance as k value changes.

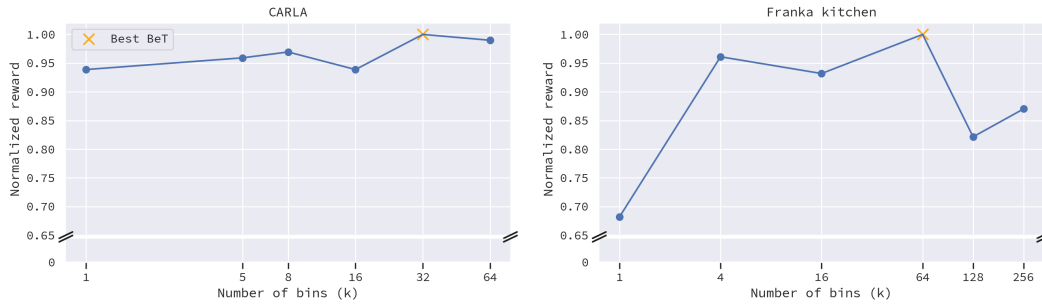


Figure 6: Ablating the number of discrete bin centers k for BeT. Reward is normalized with respect to the best performing model.

806 C.3 Ablating the core model in the architecture

807 To ablate the core MinGPT transformer model in the architecture, we replace it with a fully-connected
808 MLP network, an LSTM network, and a temporal convolution architecture.

809 Since generally MLP networks are not capable of taking in historical context in consideration, we
810 instead stack the last t frames of observation to pass into the MLP network. Near the beginning of a
811 trajectory, the stack of observation is zero-padded to t frames. For the intermediate layers in the MLP,
812 we keep the same width and the number of layers as the corresponding MinGPT.

813 For the LSTM network and the temporal convolution, we simply replace the MinGPT trunk with an
814 LSTM trunk and try to train the same sequence-to-sequence model with the same historical context
815 size.